IEEE Access
Multidisciplinary ⁝ Rapid Review ⁝ Open Access Journal

Received October 4, 2020, accepted October 13, 2020, date of publication October 16, 2020, date of current version October 28, 2020.

Digital Object Identifier 10.1109/ACCESS.2020.3031864

In-Situ Self-Aligned NaCl-Solution Fluidic-Integrated Microwave Sensors for Industrial and Biomedical Applications

NONCHANUTT CHUDPOOTI[1], (Member, IEEE), NATTAPONG DUANGRIT[2], (Member, IEEE), PATCHADAPORN SANGPET[3], PRAYOOT AKKARAEKTHALIN[3], (Member, IEEE), B. ULRIK IMBERG[4], IAN D. ROBERTSON[5], (Fellow, IEEE), AND NUTAPONG SOMJIT[5], (Senior Member, IEEE)

[1]Research Center of Innovation Digital and Electromagnetic Technology (iDEMT), Department of Industrial Physics and Medical Instrumentation, Faculty of Applied Science, King Mongkut's University of Technology North Bangkok, Bangkok 10800, Thailand
[2]Faculty of Engineering, Rajamangala University of Technology Lanna, Chiang Mai 50300, Thailand
[3]Department of Electrical and Computer Engineering, Faculty of Engineering, King Mongkut's University of Technology North Bangkok, Bangkok 10800, Thailand
[4]Huawei Technologies Sweden AB, 164 40 Kista, Sweden
[5]School of Electronic and Electrical Engineering, University of Leeds, Leeds LS2 9JT, U.K.

Corresponding author: Nutapong Somjit (n.somjit@leeds.ac.uk)

This work was supported in part by the Thailand Research Fund and Office of the Higher Education Commission through the Research Grant for New Scholar under Grant MRG6280119, in part by the King Mongkut's University of Technology North Bangkok under Contract KMUTNB-64-KNOW-44, and in part by the Engineering and Physical Science Research Council under Grant EP/S016813/1 and Grant EP/N010523/1.

ABSTRACT This work presents, for the first time, an in-situ self-aligned fluidic-integrated microwave sensor for characterizing NaCl contents in NaCl-aqueous solution based on a 16-GHz bandpass combline cavity resonator. The discrimination of the NaCl concentration is achievable by determining amplitude differences and resonant frequency translations between the incident and reflected microwave signals at the input terminal of the cavity resonator based on the capacitive loading effects of the comb structure inside the cavity introduced by the NaCl solution under test. Twelve NaCl-aqueous liquid mixture samples with different NaCl concentrations ranging from 0% to 20% (0 – 200 mg/mL), which are generally exploited in most industrial and biomedical applications, were prepared and encapsulated inside a Teflon tube performing as a fluidic channel. The Teflon tube is subsequently inserted into the cavity resonator through two small holes, fabricated through the sidewalls of the cavity, which can be used to automatically align the fluidic subsystem inside the combline resonator considerably easing the sensor setup. Based on at least five repeated measurements, the NaCl sensor can discriminate the NaCl content of as low as 1% with the measurement accuracy of higher than 96% and the maximum standard deviation of only 0.0578. There are several significant advantages achieved by the novel NaCl sensors, e.g. high accuracy, traceability and repeatability; ease of sensor setup and integration to actual industrial and biomedical systems enabling in-situ and real-time measurements; noninvasive and noncontaminative liquid solution characterization as well as superior sensor reusability due to a complete physical separation between the fluidic and microwave subsystems.

INDEX TERMS Microwave sensors, liquid material characterization, fluidic integration, combline resonators.

I. INTRODUCTION

Recently, microwave sensors and characterizations have become a popular technique for fluidic and liquid-mixture concentration sensing in various industrial applications, e.g. high-pressure liquid measurements [1], [2], material moisture content characterizations [3]–[6], continuous process monitoring of biogas plants [7], [8] and determinations of moisture content in soil [5], [9]–[11]. Moreover, they have also been proven very useful in many healthcare and biomedical

The associate editor coordinating the review of this manuscript and approving it for publication was Wuliang Yin.

applications, e.g. real-time monitoring of glucose in diabetic patients [12]–[15] and noninvasive monitoring of medical fluidic contents [12], [14], [16]. Normally, microwave sensors offer many advantages compared to other conventional liquid and fluidic sensors such as nondestructive and noninvasive measurements and, principally, requiring no additional chemicals to be added into the systems [17], [18].

NaCl-aqueous solutions play a significant role in many chemical processes in a wide variety of chemical and biological applications. Highly sensitive detection of NaCl concentration in aqueous solution may become a powerful technique for studying many useful biological properties of various liquid materials [19]–[23]. There are several techniques for sensing or classifying NaCl contents in liquid solutions. Conventional techniques for monitoring the composition of aqueous solutions include standard UV/Vis/NIR measurements [24], [25], ion-sensitive electrodes and amperometric sensors [26]–[28]. However, these techniques take a long processing and measurement time to classify the content of the NaCl in the liquid solution and require additional chemical material for determining the content of the NaCl. Commercial instruments have allowed characterizations of NaCl concentration with sufficient accuracy, for example; the micro-Raman spectroscopy technique allows the determination of the NaCl concentration of an aqueous solution with an error of approximately ±5% [29]. The spectroscopy is, however, an expensive instrument that requires specialized personnel training. With microwave measurement techniques, there are several methods to indicate liquid ingredients from liquid-mixture solutions, e.g., resonance frequency [18], [30]–[32], transmission level [17], [32], [33], phase and quality factor (*Q*-factor) [23]. Various liquid-mixture sensors based on microwave technologies have been extensively investigated, such as split-ring resonator [34]–[36], complementary split-ring resonator (CSRR) structures [17], [31], [32], [37], [38], interdigital structures [8], substrate integrated-waveguide (SIW) structures [18], waveguide structures [30] and mushroom-like structures [23]. These techniques offer a good measurement accuracy [17], [18], [31], with, generally, nondestructive measurement and short assay time.

This article presents a cavity-based combline microwave sensor for highly accurate characterizations of the NaCl concentration in an aqueous-based liquid-mixture solution. The novel sensor is designed based on a combline structure operating at 16 GHz, chosen as the best compromise between measurement sensitivity of the sensor and signal losses in the liquid mixture at various NaCl concentrations. The sensor can detect the percent concentration of NaCl in the liquid mixture by determining the amplitude and frequency translations of the incident and reflected microwave signals at the input port of the compline cavity resonator. Twelve solution samples of NaCl in aqueous-based liquid mixture, i.e. 1% (10 mg/mL), 2% (20 mg/mL), 3% (30 mg/mL), 4% (40 mg/mL), 5% (50 mg/mL), 6% (60 mg/mL), 7% (70 mg/mL), 8% (80 mg/mL), 9% (90 mg/mL), 10% (100 mg/mL), 15% (150 mg/mL) and 20% (200 mg/mL), respectively, were measured to demonstrate the performance of the sensor. The measured reflection coefficients, S_{11}, were collected and numerically evaluated for the accurate percentage of the NaCl content in the solution. The numerically calculated results from the measured datasets show a good agreement of higher than 96%, when compared with reference NaCl-aqueous liquid-mixture solutions that

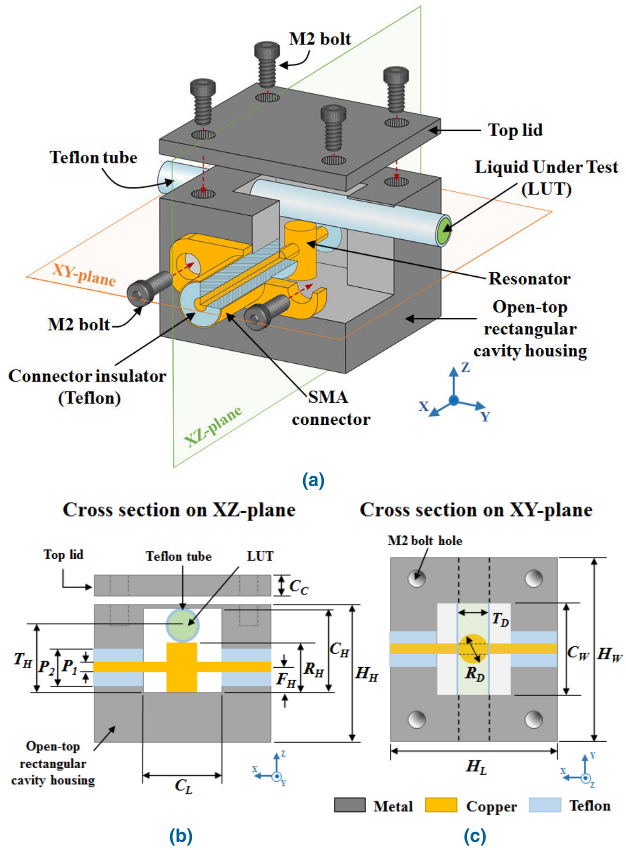

FIGURE 1. Sketches of the NaCl combline resonator sensor (a) 3D perspective view, (b) cross-section on *XZ*-plane and (c) cross-section on *XY*-plane.

TABLE 1. Microwave cavity sensor geometry.

Parameter	Description	Optimum value (mm)
C_C	Thickness of the top lid and bottom lid	2.50
C_H	Inner height of the cavity	8.80
C_L	Inner length of the cavity	10.0
C_W	Inner width of cavity	8.00
F_H	Feeding height	3.00
H_H	Housing height	11.5
H_L	Housing length	20.0
H_W	Housing width	18.0
P_1	Feeding diameter	1.30
P_2	Feeding insulator diameter	4.35
R_D	Diameter of the resonator	3.00
R_H	Height of the resonator in cavity area	4.95
T_D	Diameter of Teflon tube	3.00
T_H	Height between center of Teflon tube and cavity housing	7.15

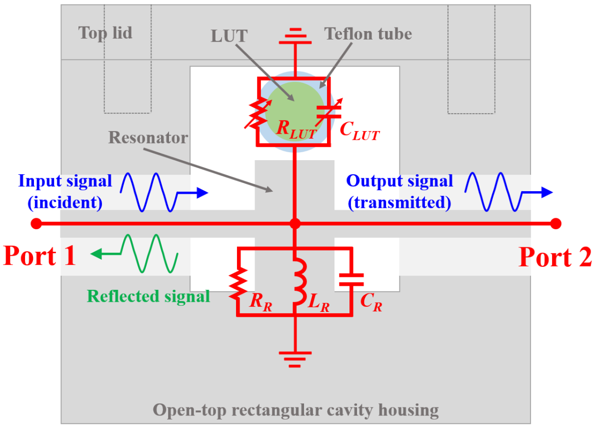

FIGURE 2. Equivalent circuit model of the NaCl cavity sensor.

were prepared in an environmentally controlled laboratory. The novel NaCl sensor achieves several significant advantages, as compare to conventional NaCl sensors, e.g. high accuracy, traceability and repeatability; ease of sensor setup and integration to actual industrial and biomedical systems, enabling in-situ and real-time measurements; nondestructive and noncontaminative liquid solution characterization as well as superior sensor reusability due to a complete physical separation between the fluidic and microwave subsystems.

II. WORKING PRINCIPLE, SENSOR DESIGN AND FABRICATION

The complete NaCl sensor system, as shown in Fig. 1 (a), consists of two different subsystems: a fluidic subsystem using a Teflon tube to encapsulate the NaCl-aqueous liquid mixture solution under test and a 16-GHz custom-made combline cavity resonator performing as the microwave sensing subsystem. The microwave cavity resonator is composed of three parts, which are the open-top rectangular cavity housing, the top lid as the metallic cover on top of the cavity housing and the cylindrical combline structure at the center inside the cavity. The operational frequency of 16 GHz is selected as the best compromise between various key parameters such as sensor sensitivity, size, fabrication cost and etc. The Teflon tube, performing as the liquid encapsulation channel, is mounted into the rectangular cavity resonator by two pilot etched-through holes embedded into two sidewalls of the cavity. The pilot holes are also used to precisely align and firmly positioned the Teflon tube to be on top of the combline resonator achieving the best sensor sensitivity and mechanical reliability.

A. WORKING PRINCIPLE

Figure 2 presents the equivalent circuit model of the combline cavity resonator sensor integrated with the fluidic subsystem. An incident microwave signal is injected at the input terminal, port 1, and propagates towards the combline resonator, presented as the parallel R_R, L_R and C_R, located at the center of the rectangular cavity structure. The propagating incident electromagnetic (EM) wave is subsequently modulated by the NaCl liquid-mixer solution encapsulated inside the Teflon tube mounted firmly on top of the combline resonator. The encapsulated NaCl-aqueous solution can be represented with a basic variable parallel *RC*-resonant circuit with the resistor and capacitor values of R_{LUT} and C_{LUT}, respectively, depending on the NaCl concentration in the liquid mixer solution. The propagating incident microwave signal is then split into two signals, due to the impedance mismatch of the combline resonator; 1) the transmitted signal propagating towards port 2, the output terminal, and 2) the reflected signal propagating back to the input port. By measuring the reflected signal at the input terminal, the percent concentration of the NaCl in aqueous solution can be numerically computed from the amplitude attenuation and the resonant frequency shift, as compared to the incident input signal, using resonant technique [18], [31]. The EM effect of the Teflon tube in the measurement is negligible only when the combline NaCl sensor is first calibrated with an empty Teflon tube used in the measurement setup before an actual measurement with an unknown concentration of the NaCl-aqueous solution under test is performed.

B. SENSOR DESIGN AND OPTIMIZATION

The fluidic-integrated combline-resonator sensor, based on the hollow rectangular cavity structure, was designed and optimized by using a 3D full-wave EM simulator, namely CST Studio Suite [39]. Figures 1 (b) and (c) show the cross-section visualizations on the *XZ* and *XY*-planes of the NaCl combline resonator sensor, respectively. The combline-resonator sensor was designed at the center frequency, f_0, of 16 GHz, bandwidth, f_c, of 1 GHz and passband ripple of 0.5 dB. To ease the sensor design and fabrication, the order of the resonator is fixed to n = 1. The Chebyshev *g*-values for 1^{th} order filter with 0.5-dB ripple [40] is $g_0 = 1.00$, $g_1 = 0.6986$ and $g_2 = 1.00$. The Chebyshev *g*-values were used to calculate the initial physical dimensions of the cavity resonator [41]. However, due to fabrication limitations of the manufacturing facility, the diameter of combline resonator, R_D, was selected to 3.00 mm. The height of the combline resonator, R_H, is numerically optimized, by using parametric sweep process, to 4.95 mm. The optimized resonator height of 4.95 mm is initially calculated to be approximately at $\lambda_g/4$, where λ_g is the guided wavelength of the EM waves propagating inside the hollow cavity at the operational frequency of 16 GHz. The cylindrical combline resonator is designed and located at the center of the rectangular cavity. The inner dimensions of the hollow rectangular cavity housing is calculated and optimized based on basic combline bandpass filter design theory [41] to the length = 10.00 mm (C_L)× width = 8.00 mm (C_W)× height = 8.80 (C_H), which can be precisely manufactured into the cavity housing block during the fabrication process. The input and output ports are connected to the combline structure by inductive feeding technique to couple the EM waves between the feed networks to the combline resonator. In the simulations, the feeding

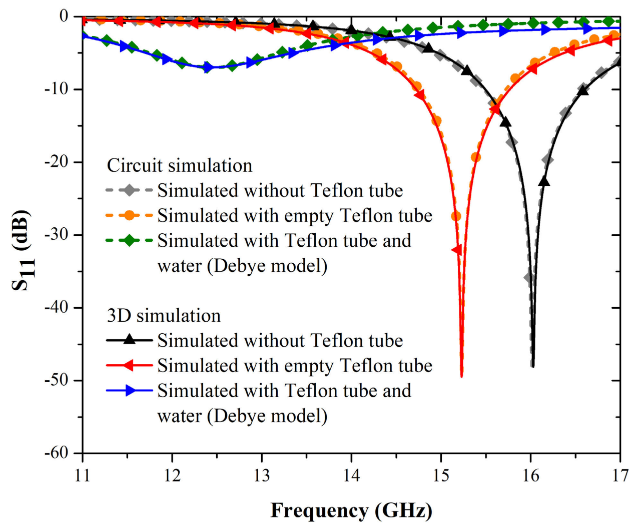

FIGURE 3. Simulated reflection coefficient, S_{11}, comparisons between circuit and 3D EM modeling of the NaCl cavity sensors with three different scenarios: 1) cavity sensor design without a Teflon tube, 2) cavity sensor design integrated with an empty Teflon tube and 3) cavity sensor design integrated with a water-filled Teflon tube.

networks are modelled by using the SMA feed launchers [42] on both sides of the combline resonators, introducing the best-possible actual sensor physical geometry and measurement setup simulations. The feeding height, F_H, is designed and optimized to 3.00 mm from bottom part of the combline cavity structure considering also the physical limitation of the fabrication process. In the simulations, a Teflon tube with dielectric constant of 2.0 is used and modelled as the fluidic channel encapsulating NaCl-aqueous liquid mixer under test. The Teflon fluidic channel is located on top of the combline resonator for maximum EM interaction between the NaCl liquid mixer under test and the electric field introduced by the combline structure. The outer diameter of the Teflon tube of 3.00 mm with the Teflon wall thickness of 1.00 mm is portrayed in the simulation. The top lid of the hollow rectangular cavity resonator is modelled using a steel plate with the thickness of 2.5 mm in the designs. The optimum values of all design parameters are listed in Table 1.

Figure 3 show the compared results between the circuit simulation and 3D simulation of the NaCl sensor with three different scenarios: 1) cavity sensor design, 2) cavity sensor design integrated with hollow Teflon channel and 3) cavity sensor design integrated with water-filled Teflon tube. For the 3D structure simulation, the first scenario, the operating frequency of the cavity combline resonator is approximately 16.04 GHz. After modeling the empty Teflon tube on top of the combline resonator, second scenario, the simulated operating frequency is shifted to approximately 15.24 GHz. For the third simulation scenario, the water is filled and encapsulated in the Teflon tube and modelled by Debye technique included in the software simulation package. The simulated operating frequency for this case is subsequently shifted to approximately 12.40 GHz. To validate the equivalent circuit

TABLE 2. Values of the discrete components in the equivalent circuit model of the NaCl cavity sensor (Fig. 2).

Design scenarios	R_R (Ω)	L_R (pH)	C_R (pF)	R_{LUT} (Ω)	C_{LUT} (pF)
Cavity sensor without a Teflon tube	13,800	49.675	1.987	-	-
Cavity sensor with an empty Teflon tube	13,800	49.675	1.987	70,000	0.21
Cavity sensor with a water-filled Teflon tube	13,800	49.675	1.987	31	1.30

model in the Fig. 2, the value of R_R, L_R, C_R, R_{LUT} and C_{LUT}, optimized by commercial 3D full-wave EM simulator (CST Studio suite) at the nominal operating frequency with three different scenarios: 1) cavity sensor without a Teflon tube, 2) cavity sensor integrated with an empty Teflon tube and 3) cavity sensor design integrated with a water-filled Teflon tube. All values of the equivalent circuit models are shown in Table 2. The resonant frequency is clearly modulated and shifted to lower values due to higher effective dielectric constants of the measurement environment inside the hollow rectangular cavity sensor. Therefore, the NaCl content in the aqueous-based liquid-mixture can be accurately determined using the resonant frequency shift, S_{11}, compared between the sensor with empty Teflon tube and the same tube encapsulated with liquid mixture.

C. NaCl CAVITY SENSOR FABRICATION AND ASSEMBLY

The rectangular cavity structure is composed of bottom and top lids, and hollow rectangular cavity housing as shown in Figure 4 (a). All parts of the rectangular cavity are fabricated from steel blocks using subtractive manufacturing with the LPKF ProtoLaser U3. The bottom lid of the hollow rectangular cavity was patterned using a 2.50-mm-thick, C_C, steel block with the length $=$ 20 mm (H_L)$\times$ width $=$ 18.0 mm (H_W). Four M2 screw holes used to align the position of the rectangular cavity were drilled near four corners of the bottom lid steel block. At the center of the bottom lid, another etch-through M3 screw hole with the diameter of 3.00 mm was drilled for mounting the combline resonator structure. The cylindrical combline resonator was fabricated from a copper block using the CNC machine. The fabricated diameter of the copper rod structure was 3.00 mm with the height of 4.95 mm. The hollow rectangular cavity housing was fabricated of a steel block with dimensions of the length $=$ 20.00 mm (H_L)$\times$ width $=$ 18.0 mm (H_W)$\times$ height $=$ 8.80 mm (H_H) using the LPKF ProtoLaser U3. The inner dimensions of the rectangular cavity were: length $=$ 10.00 mm (C_L) $\times$ width $=$ 8.00 mm (C_W)$\times$ height $=$ 8.80 (C_H). Near the four corners of the rectangular cavity housing, the M2 screw holes were drilled through to mount the top and bottom lids. Two side walls of the hollow rectangular cavity housing were etched through for connecting the SMA connectors injecting EM signals from the network analyzer into the cavity sensor. The diameter of the SMA etch-through

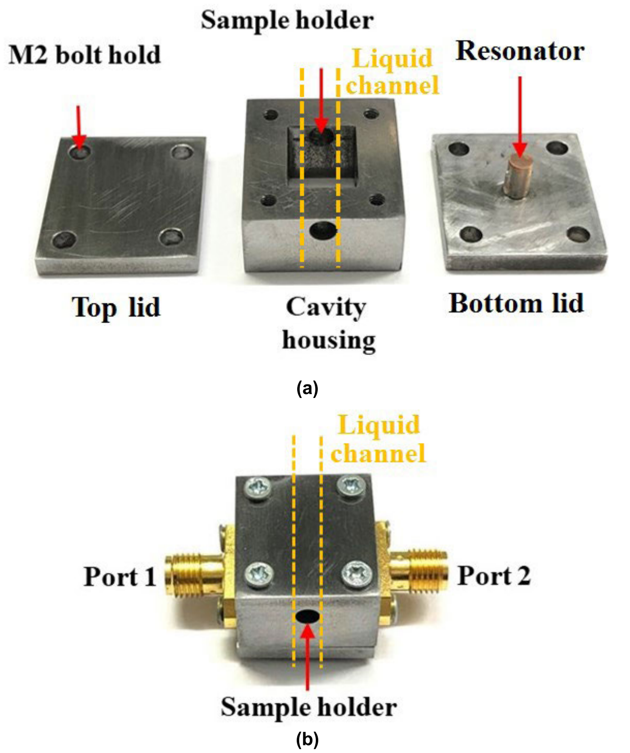

FIGURE 4. **(a) Fabricated NaCl sensor prototype before assembly, which composed of the hollow rectangular housing and its top and bottom steel lids. (b) Assembled NaCl sensor prototype without Teflon tube.**

hole, P_2, is 4.35 mm. The other two side walls of the rectangular cavity housing were also etched through, with the diameter of 3.00 mm, used for inserting the Teflon tube. The drilling distance, T_H, between the pilot-holes guiding the Teflon tube and the bottom plane of the rectangular hollow housing was 7.15 mm. Finally, the top lid of the hollow rectangular cavity housing was fabricated from 2.50-mm-thick, C_C, steel block with length = 20 mm (H_L)× width = 18.0 mm (H_W). Close to the four corners of the top lid, four M2 screw holes with a diameter of 2 mm were drilled through and used to attach the top lid to the cavity housing. The Fig. 4(b) shows the assembled NaCl rectangular cavity sensor prototype with two SMA connectors and without Teflon tube fluidic channel.

D. NaCl SOLUTION PREPARATION

All NaCl solutions were prepared in the environmentally controlled chemistry laboratory with the temperature of 25 °C and the relative humidity of 50%. The NaCl solutions were mixed from 99.5% NaCl powder and DI water, which had an electrical resistivity of more than 10 MΩ-cm. All glass beakers and test tubes used in the liquid preparation were first cleaned from organic contaminations using acetone and isopropanol ensuring that no other organic substances will affect the S-parameter measurement. Twelve NaCl-H_2O solutions were selected and mixed as NaCl-aqueous solution under test. The NaCl content in the liquid mixer under test was varied in the range of 1% (10 mg/mL), 2% (20 mg/mL), 3% (30 mg/mL), 4% (40 mg/mL), 5% (50 mg/mL), 6% (60 mg/mL), 7% (70 mg/mL), 8% (80 mg/mL), 9% (90 mg/mL), 10% (100 mg/mL), 15% (150 mg/mL) and 20% (200 mg/mL) by mixing the NaCl power to the DI water as follows:

1. A 3-digit electronic precision balance was used to weigh 30 grams of NaCl powder to be mixed with 150-ml DI water, creating the initial NaCl liquid substance at 20%w/v (200 mg/mL) NaCl liquid mixer, C_1.
2. The liquid dilution technique was used to prepare the lower NaCl concentrations by mixing the 20%w/v (200 mg/mL) initial NaCl substance with different volumes of DI water as shown in Table 2. The formula of the dilution method is calculated by:

$$C_1 V_1 = C_2 V_2 \tag{1}$$

where, C_1: initial concentration, V_1: initial volume, C_2: final targeted concentration, V_2: final targeted volume.

3. Preparation of the targeted concentration of the NaCl solution, C_2, and the required volume of the initial NaCl solution, V_1, by fixing the total targeted volume to the required NaCl concentration, V_2, at 10 ml. The values of C_2, V_1, and the DI water volume in each NaCl solution are calculated and shown in the Table 3.
4. The required volume of the initial NaCl solution, V_1, and the DI water volume were diluted and mixed into the test tube by using the digital micropipette for high precision level of NaCl liquid solutions.

III. MEAUREMENT RESULTS

A. MEASUREMENT SETUP

The S-parameter measurements were performed by using a ROHDE & SCHWARZ ZVB-20 Vector Network Analyzer (VNA). Two-port calibration technique was performed using the Thru-Open-Short-Match method (TOSM), in order to eliminate the systematic errors contributed by the VNA and connecting cables. The frequency range of the VNA was set from 10 GHz to 17 GHz. The number of sampling frequency points was 7,001 points. The intermediate frequency (IF) filter bandwidth was set to 100 Hz. To accurately feed the Teflon tube with the NaCl solution under test, the liquid solution was carefully injected into the liquid channel by using an industrial grade syringe, ensuring that no air bubbles were trapped inside in the encapsulated liquid channel during the sensor measurement. The temperature of the liquid solution sample was well maintained at a room temperature of 25 °C. At least five repeated individual measurements were conducted to ensure the measurement and sensor repeatability. Fig. 5 shows the measurement setup of the NaCl sensors integrated with Teflon fluidic channel. Fig. 6 compare the S_{11} measurement results to the simulation results of the NaCl sensor with and without the empty Teflon tube, respectively.

B. DI-WATER/NaCl LIQUID MIXTURE MEASUREMENT

The verification of the NaCl concentration was investigated using different concentrations of the NaCl and DI water mixture. The concentration of NaCl solution in DI water varied

TABLE 3. **The calculated volumes of the NaCl solutions, V_1 and the DI water by using dilution method for the targeted NaCl concentrations.**

Initial NaCl solution, C_1	Required volume of the initial NaCl solution, V_1	Targeted NaCl concentration, C_2 (%w/v)	Liquid mixer volume at Targeted NaCl concentration, V_2	DI water volume used to dilute the initial NaCl solution, $V_2 - V_1$
Following step 1: @20% NaCl	0.5 ml.	1% (10 mg/mL)	Fixed@10 ml.	9.5 ml.
	1.0 ml.	2% (20 mg/mL)		9.0 ml.
	1.5 ml.	3% (30 mg/mL)		8.5 ml.
	2.0 ml.	4% (40 mg/mL)		8.0 ml.
	2.5 ml.	5% (50 mg/mL)		7.5 ml.
	3.0 ml.	6% (60 mg/mL)		7.0 ml.
	3.5 ml.	7% (70 mg/mL)		6.5 ml.
	4.0 ml.	8% (80 mg/mL)		6.0 ml.
	4.5 ml.	9% (90 mg/mL)		5.5 ml.
	5.0 ml.	10% (100 mg/mL)		5.0 ml.
	7.5 ml.	15% (150 mg/mL)		2.5 ml.
	10.0 ml.	20% (200 mg/mL)		0.0 ml.

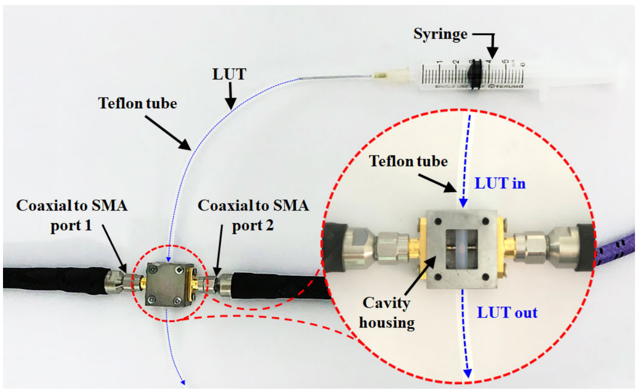

FIGURE 5. **Fabricated sensor after injecting the liquid solution sample into the Teflon tube and connecting the sensor to the coaxial cable and that to the VNA.**

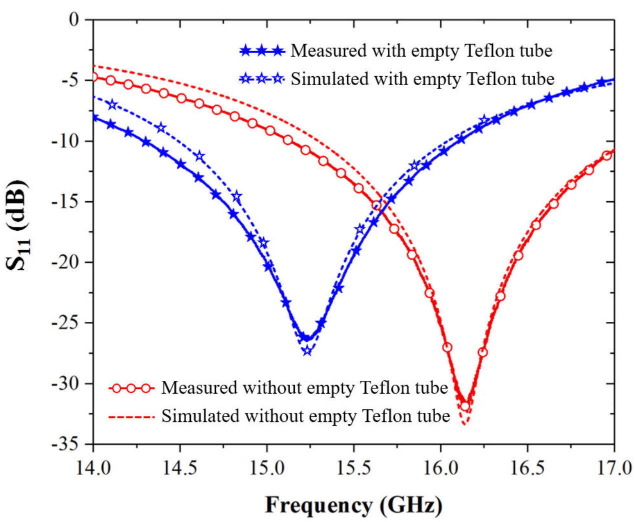

FIGURE 6. **Simulated (dashed line) and measured (solid line) reflection coefficients, S_{11}, of the NaCl cavity sensor with and without an empty Teflon tube.**

from 0% – 20% (0 – 200 mg/mL). The 0% NaCl is DI water, which is the reference liquid solution. The full measurement consists of the following steps:

1. Measure the reflection coefficient, S_{11}, with DI water as the reference measurement.

2. Measure the reflection coefficient, S_{11}, with different concentration of the NaCl and calculate the resonant frequency change from $|\Delta f_r| = |f_{(\%NaCl)} - f_{(DI\ water)}|$.

3. Re-measure with same concentration of the NaCl five times to find the accuracy of the measurement.

The measured data were collected five times for each liquid solution to ensure the repeatability of the proposed sensor. The corresponding S_{11} measurements of these samples are shown in Fig. 8. Due to the small difference in resonant frequency between each liquid solution, the traces for the odd and even concentrations of the NaCl solution in DI water are separated into Fig.7(a) and Fig.7(b), respectively, for clarity.

As discussed, injecting the NaCl solution sample into the microwave cavity sensor causes the resonant frequency to shift towards and the return loss to decrease when compared with DI water as a reference measurement. When comparing the lowest percentage, 1% (10 mg/mL), of NaCl in liquid mixture, with DI water as a reference measurement, the minimum shift in resonant frequency is observed to be 31 MHz. On the other hand, the maximum shift in resonant frequency is 616 MHz, for the 20% (200 mg/mL) NaCl solution. A plot of difference in resonant frequency, Δf_r, as a function of percentage of NaCl in the liquid mixture is shown in Fig. 8. To validate the numerical equation for extracting the percentage of NaCl in liquid mixture, all values of the difference resonant frequencies, Δf_r, are fitted to a polynomial using the commercial data analysis and visualization software package Origin. A 3rd order polynomial was used, yielding regression value R^2 of 0.9997. The polynomial itself was found to be:

$$\%NaCl = 7.854 \times 10^{-8} (\Delta f_r)^3 - 4.478 \times 10^{-5} (\Delta f_r)^2 + 2.985 \times 10^{-2} (\Delta f_r) + 0.109 \quad (2)$$

where $\%NaCl$ is the percentage of NaCl in the liquid mixture and the change in resonant frequency, Δf_r, has units of MHz. A summary of the measured and extracted data is given in Table 4. A good agreement is observed between the extracted and known concentration of NaCl in the

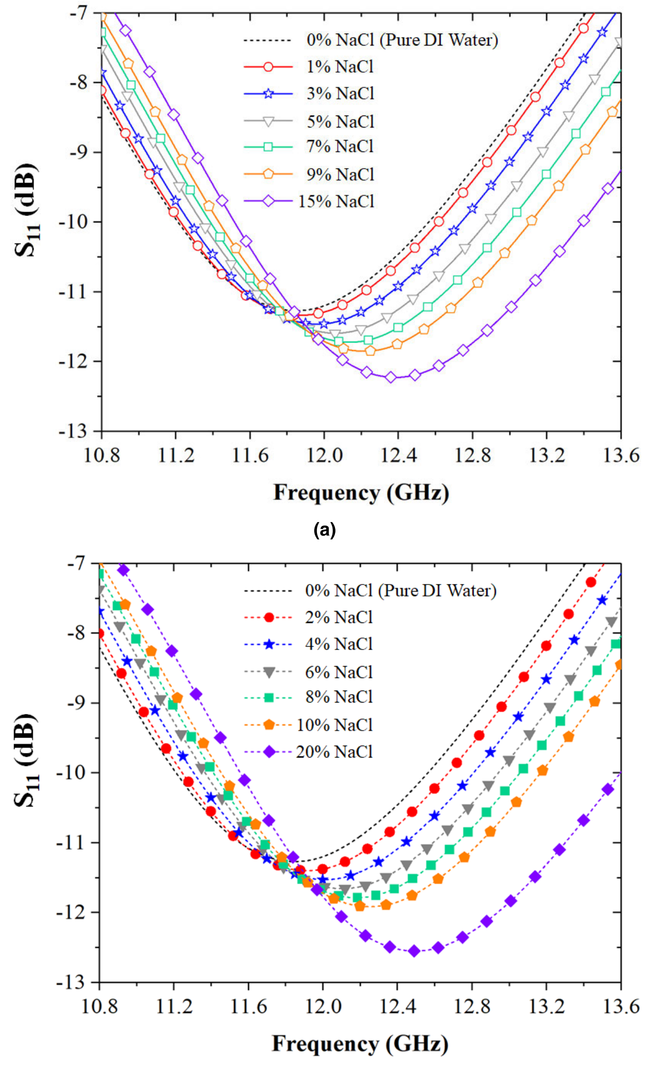

FIGURE 7. Measured reflection coefficient, S_{11}, in dB for NaCl concentration in the range from 0% to 20%. (a) the magnitude of S_{11} for NaCl concentration in the range of 0%, 1% (10 mg/mL), 3% (30 mg/mL), 5% (50 mg/mL), 7% (70 mg/mL), 9% (90 mg/mL) and 15% (150 mg/mL) in DI water and (b) the magnitude of S_{11} for NaCl concentration in the range of 0%, 2% (20mg/mL), 4% (40 mg/mL), 6% (60 mg/mL), 8% (80 mg/mL), 10% (100 mg/mL) and 20% (200 mg/mL) in DI water.

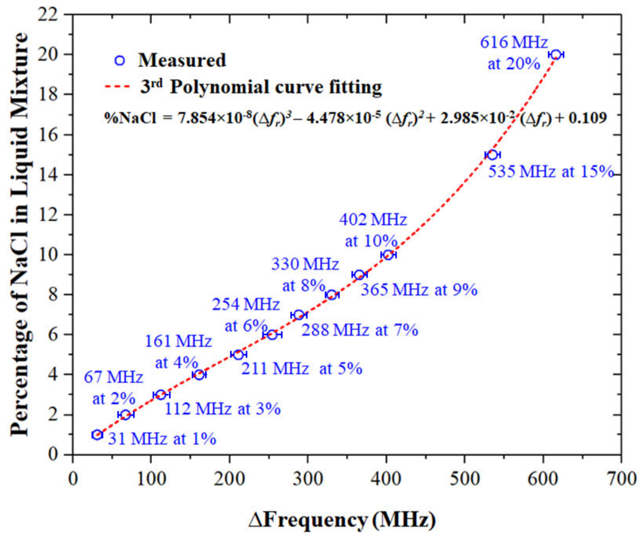

FIGURE 8. Percentages of NaCl concentration in H_2O-NaCl liquid mixture fitted as a function of resonant frequencies in MHz. The regression value and fitted polynomial (dashed line) were calculated by Origin.

TABLE 4. Extracted results of various concentration of NaCl.

%NaCl	Relative resonant frequency, Δf_r, (MHz)	Extracted *%NaCl* from Eqn. (3)	%Difference
1	31	0.994	0.63
2	67	1.932	3.42
3	112	3.001	0.03
4	161	4.082	2.05
5	211	5.151	3.03
6	254	6.089	1.48
7	288	6.868	1.89
8	330	7.905	1.18
9	365	8.858	1.58
10	402	9.974	0.26
15	535	15.288	1.92
20	616	19.863	0.69

liquid mixture. The biggest difference in %NaCl was only 3.42%. This shows that the sensor retains the accuracy offered by the resonance technique. Table 5 shows the key parameters of the microwave cavity sensor compared with other published works, [16], [19]–[21], [44]. The key advantages of the proposed sensor are the real-time monitoring, ease of center setup and integrated with the system, self-alignment between fluidic channel and microwave system, and unlimited life-cycle limitation. The self-aligned fluidic channel criteria, which is crucial key for sensor setup, was listed in Table 5. In [19] and this work, the liquid channel is integrated into the system to reduce the measurement error from measurement setup. To implement the sensor with industrial or biomedical applications, the proposed sensor can easily integrate with the system when compared with other publishes [16], [19]–[21], [44] because other works need to modify the cover structure to protect the RF signal environment generation.

C. SENSOR REPEATABILITY AND LIMITATIONS

To measure the repeatability of the sensor, two experiments were performed. Firstly, the liquid samples were injected five times without any changes the system. The standard deviation of these measurements was calculated. The minimum, maximum and average standard deviations of the measured reflection coefficient, S_{11}, were 0.0017, 0.0578 and 0.0244, respectively. Secondly, the proposed sensor is taken out and re-mounted at both SMA ports (port 1, port 2) and the measurement repeated five times. The minimum, maximum and average of the standard deviation of measured the reflection coefficient, S_{11}, were 0.0046, 0.0713 and 0.0367, respectively.

TABLE 5. Key factor comparison of measurement of this work and other works.

Key factor	[20]	[16]	[19]	[21]	[44]	***This work***
Percentage of NaCl discrimination	20 %w/v (200 mg/mL)	20%w/v (200 mg/mL)	2%w/v (20 mg/mL)	1%w/v (10 mg/mL)	0.1%w/v (1 mg/mL)	***1%w/v (10 mg/mL)***
Operating frequency	860 – 960 MHz	4.3 GHz	8.4 GHz	1.9 – 2.1 GHz	~1.9 GHz	***16 GHz***
Sensitivity	N/A	N/A	N/A	0.069 dB/(g/L) @ 0 – 10 g/L 0.082 dB/(g/L) @ 10 – 100 g/L	0.1 $(g/L)^{-1}$	***0.237 (g/L)/MHz @ 10 – 100 g/L 0.458 (g/L)/MHz @100 – 200 g/L***
Characterization technique	Received power level (dBm)	Reflection amplitude	Transmission coefficient	Transmission coefficient	Transmission coefficient	***Resonant frequency***
Sensor structure	RFID tag	Circular patch on planar structure	Interdigitated capacitor	Hairpin resonator on planar structure	*LC* resonator loaded to a microstrip	***Combline cavity resonator***
Design complexity	Low	Low	Moderate	Low	Moderate	***Moderate***
Fabrication technique	Milling machine	Milling machine	Cleanroom	Milling machine	Milling machine & Chemical process	***Milling machine & Photolaser machine***
Fabrication cost	Low	Low	High	Low	Moderate	***Low***
Fabrication complexity	Low (require fabrication only for microwave part)	Low (require fabrication only for microwave part)	High (require high precision fabrication of microwave and microfluidic parts)	Low (require fabricating only microwave sensor part)	Moderate (require fabrication for both microwave and microfluidic parts)	***Low (require fabrication only for microwave part)***
Self-aligned fluidic channel	No	No	Yes	No	No	***Yes***
Ease of measurement setup	No	No	No	No	Yes	***Yes***
Real time and In-situ measurement	Difficult (required structural modification)	Incapable	Difficult (required structural modification)	Difficult (required structural modification)	Difficult (required structural modification)	***Easy***
Reusability	Yes	No	No	Yes	Yes	***Yes***
Repeated measurements/repeatability	1 time	1 time	1 time	1 time	1 time	***5 times***

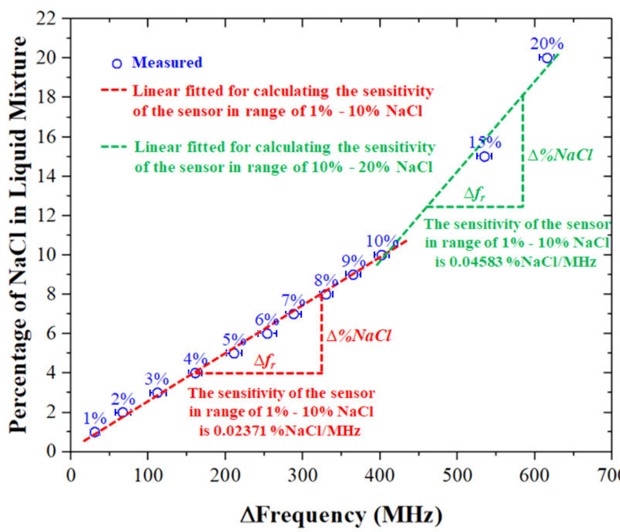

FIGURE 9. Two piecewise linear fitted plots for calculating the sensitivity of the proposed sensor in range of 1% - 20% (10 – 200 mg/mL) NaCl in the liquid mixture.

The sensitivity of the sensor to the percentage of NaCl in the liquid solution can be determined as the ratio between the change of %NaCl and the difference in the resonant frequency – in other words, the slope of the transfer function in Fig. 9. Due to the non-linear function, two sections, e.g., the percentage of the NaCl in the range of 1% – 10% (10 – 100 mg/mL) and 10% – 20% (100 – 200 mg/mL), are characterized. The sensitivity of the percentage of NaCl in liquid mixture in range of 1% – 10% (10 – 100 mg/mL) and 10% – 20% (100 – 200 mg/mL) were 0.02371 %NaCl/MHz (0.2371 g/L/MHz) and 0.04583 %NaCl/MHz (0.4583 g/L/MHz), respectively. However, to compare the sensitivity of this sensor with other works, the normalized sensitivity [43] was calculated to 0.487%.

For the limitation of the proposed sensor for %NaCl determination, in this article, the microwave cavity sensor can be detected every 1% (10 mg/mL) of the NaCl in the liquid mixture. However, the minimum measurement percentage of the NaCl in the liquid solution depends on resolution in the measurement setup. The frequency range of VNA was set from 10 GHz to 17 GHz. The number of points was 7,001. Using this measurement setup, a minimum frequency shift of 1 MHz can be determined. The resolution can be calculated by using Eqn. (2). Substituting the value of Δf_r with 1 MHz, from the measurement setup, shows that the smallest percentage change of NaCl concentration that can be theoretically detected is 0.14% (1.4 mg/mL). On the other hand, the maximum percentage of the NaCl is 36% (360 mg/mL) due to saturated point of NaCl in DI water at room temperature. However, the number of points of the network analyzer can be set to a maximum of 60,0001 points. The higher number of points will affect the measurement time, however. In this article, 7,001 points were used as the best compromise between measurement time and resolution of the sensor due to the equipment available in the laboratory.

IV. CONCLUSION

A microwave cavity sensor for DI water/NaCl liquid-mixture characterization, operating at 16 GHz, has been proposed and its performance investigated. A single rod comb-line cavity sensor was found to be sufficient to classify the percentage of NaCl in the liquid mixture with a step of 1%. The extracted liquid content of NaCl results from the develop numerical model show an excellent agreement of higher than 96% when compared with NaCl solutions which were prepared in the laboratory. Further advantages of the proposed sensor are reduced measurement time, ease of operation, and contactless operation. Finally, the frequency range of the sensor can be readily extended to higher bands, improving its resolution.

ACKNOWLEDGMENT

The authors would like to thank Mr. Augustus Boadu for his contributions in preliminary investigation of fluidic-integrated combline resonator sensors.

REFERENCES

[1] W. Zhu, B. Cheng, Y. Li, R. Nygaard, and H. Xiao, "A fluidic-based high-pressure sensor interrogated by microwave Fabry–Pérot interferometry," *IEEE Sensors J.*, vol. 17, no. 14, pp. 4388–4393, Jul. 2017.

[2] C. Schuster, P. Schumacher, M. Schusler, A. Jimenez-Saez, and R. Jakoby, "Passive chipless wireless pressure sensor based on dielectric resonators," in *Proc. IEEE SENSORS*, Glasgow, U.K., Oct. 2017, pp. 1–3.

[3] Y. Wu, G. Tian, and W. Liu, "Research on moisture content detection of wood components through Wi-Fi channel state information and deep extreme learning machine," *IEEE Sensors J.*, vol. 20, no. 17, pp. 9977–9988, Sep. 2020, doi: 10.1109/JSEN.2020.2989347.

[4] J. Zhang, D. Du, Y. Bao, J. Wang, and Z. Wei, "Development of multifrequency-swept microwave sensing system for moisture measurement of sweet corn with deep neural network," *IEEE Trans. Instrum. Meas.*, vol. 69, no. 9, pp. 6446–6454, Sep. 2020, doi: 10.1109/TIM.2020.2972655.

[5] R. R. Mohan, A. Pradeep, S. Mridula, and P. Mohanan, "Microwave imaging for soil moisture content estimation," in *Proc. IEEE Int. Symp. Antennas Propag. (APSURSI)*, Fajardo, Puerto Rico, Jun. 2016, pp. 865–866.

[6] S. Seewattananpon, N. Promasa, N. Chudpooti, and P. Akkaraekthalin, "Paddy moisture measurement system in hopper silo by using near-field transmission technique," in *Proc. Int. Symp. Antennas Propag. (ISAP)*, Busan, South Korea, Oct. 2018, pp. 1–2.

[7] T. Nacke, A. Barthel, C. Pflieger, U. Pliquett, D. Beckmann, and A. Goller, "Continuous process monitoring for biogas plants using microwave sensors," in *Proc. 12th Biennial Baltic Electron. Conf.*, Tallinn, Estonia, Oct. 2010, pp. 239–242.

[8] W. Krudpun, N. Chudpooti, P. Lorwongtragool, S. Seewattanapon, and P. Akkaraekthalin, "PSE-coated interdigital resonator for selective detection of ammonia gas sensor," *IEEE Sensors J.*, vol. 19, no. 23, pp. 11228–11235, Dec. 2019.

[9] A. Loew and W. Mauser, "On the disaggregation of passive microwave soil moisture data using a priori knowledge of temporally persistent soil moisture fields," *IEEE Trans. Geosci. Remote Sens.*, vol. 46, no. 3, pp. 819–834, Mar. 2008.

[10] T. Zhang, L. Jiang, L. Chai, T. Zhao, and Q. Wang, "Estimating mixed-pixel component soil moisture contents using biangular observations from the HiWATER airborne passive microwave data," *IEEE Geosci. Remote Sens. Lett.*, vol. 12, no. 5, pp. 1146–1150, May 2015.

[11] S. Paloscia, P. Pampaloni, E. Santi, S. Pettinato, A. Della Vecchia, P. Ferrazzoli, and L. Guerriero, "Soil moisture effect on microwave emission of forest canopies," in *Proc. Microw. Radiometry Remote Sens. Environ.*, Firenze, Italy, Mar. 2008, pp. 1–4.

[12] X. Xiao and Q. Li, "A noninvasive measurement of blood glucose concentration by UWB microwave spectrum," *IEEE Antennas Wireless Propag. Lett.*, vol. 16, pp. 1040–1043, 2017.

[13] C. G. Juan, E. Bronchalo, B. Potelon, C. Quendo, E. Ávila-Navarro, and J. M. Sabater-Navarro, "Concentration measurement of microliter-volume water–glucose solutions using *Q* factor of microwave sensors," *IEEE Trans. Instrum. Meas.*, vol. 68, no. 7, pp. 2621–2634, Jul. 2019.

[14] M. Hofmann, G. Fischer, R. Weigel, and D. Kissinger, "Microwave-based noninvasive concentration measurements for biomedical applications," *IEEE Trans. Microw. Theory Techn.*, vol. 61, no. 5, pp. 2195–2204, May 2013.

[15] G. Govind and M. J. Akhtar, "Metamaterial-inspired microwave microfluidic sensor for glucose monitoring in aqueous solutions," *IEEE Sensors J.*, vol. 19, no. 24, pp. 11900–11907, Dec. 2019.

[16] M. N. Rahman, S. A. Hassan, M. Samsuzzaman, M. S. J. Singh, and M. T. Islam, "Determination of salinity and sugar concentration using microwave sensor," *Microw. Opt. Technol. Lett.*, vol. 61, no. 2, pp. 361–364, Nov. 2018.

[17] N. Chudpooti, E. Silavwe, P. Akkaraekthalin, I. D. Robertson, and N. Somjit, "Nano-fluidic millimeter-wave Lab-on-a-Waveguide sensor for liquid-mixture characterization," *IEEE Sensors J.*, vol. 18, no. 1, pp. 157–164, Jan. 2018.

[18] E. Silavwe, N. Somjit, and I. D. Robertson, "A microfluidic-integrated SIW Lab-on-Substrate sensor for microliter liquid characterization," *IEEE Sensors J.*, vol. 16, no. 21, pp. 7628–7635, Nov. 2016.

[19] T. Chretiennot, D. Dubuc, and K. Grenier, "Bi-frequency-based microwave liquid sensor for multiple solutes quantification in aqueous solution," in *Proc. 44th Eur. Microw. Conf.*, Rome, Italy, Oct. 2014, pp. 287–290.

[20] M. A. Ennasar, O. E. Mrabet, K. Mohamed, and M. Essaaidi, "Design and characterization of a broadband flexible polyimide RFID tag sensor for NaCl and sugar detection," *Prog. Electromagn. Res. C*, vol. 94, pp. 273–283, 2019.

[21] C.-F. Liu, M.-K. Chen, M.-H. Wang, and L.-S. Jang, "Improved hairpin resonator for microfluidic sensing," *Sensors Mater.*, vol. 30, no. 5, pp. 979–990, 2018.

[22] M. O. Pedrola, O. Korostynska, A. Mason, and A. I. Al-Shamma'a, "Real-time sensing of NaCl solution concentration at microwave frequencies using novel Ag patterns printed on flexible substrates," in *Proc. J. Phys., Conf.*, vol. 450, 2013, Art. no. 012016.

[23] T. Pechrkool, N. Chudpooti, N. Duangrit, S. Chaimool, and P. Akkaraekthalin, "Zeroth-order resonator based on mushroom-like structure for liquid mixture concentration sensing of sodium chloride solution," in *Proc. IEEE Conf. Antenna Meas. Appl. (CAMA)*, Kuta, Bali, Indonesia, Oct. 2019, pp. 222–224.

[24] A. Stadler, "Analyzing UV/Vis/NIR spectra—Correct and efficient parameter extraction," *IEEE Sensors J.*, vol. 10, no. 12, pp. 1921–1931, Dec. 2010.

[25] A. Stadler, "Analyzing UV/Vis/NIR spectra—Part II: Correct and efficient parameter extraction," *IEEE Sensors J.*, vol. 11, no. 4, pp. 897–904, Apr. 2011, doi: 10.1109/JSEN.2010.2057421.

[26] N. Honda, K. Emi, T. Katagiri, T. Irita, S. Shoji, H. Sato, T. Homma, T. Osaka, M. Saito, J. Mizuno, and Y. Wada, "3-D comb electrodes for amperometric immuno sensors," in *Proc. 12th Int. Conf. Solid-State Sensors, Actuat. Microsyst. Dig. Tech. Papers (TRANSDUCERS)*, Boston, MA, USA, Jun. 2003, pp. 1132–1135, doi: 10.1109/SENSOR.2003.1216969.

[27] P. Kassanos, S. Anastasova, and G.-Z. Yang, "A low-cost amperometric glucose sensor based on PCB technology," in *Proc. IEEE SENSORS*, New Delhi, India, Oct. 2018, pp. 1–4.

[28] A. K. Samarao, M. J. Rust, and C. H. Ahn, "Rapid fabrication of a nano interdigitated array electrode and its amperometric characterization as an electrochemical sensor," in *Proc. IEEE Sensors*, Atlanta, GA, USA, Oct. 2007, pp. 644–647.

[29] I. Duričković, M. Marchetti, R. Claverie, P. Bourson, J.-M. Chassot, and M. D. Fontana, "Experimental study of NaCl aqueous solutions by Raman spectroscopy: Towards a new optical sensor," *Appl. Spectrosc.*, vol. 64, no. 8, pp. 853–857, Aug. 2010.

[30] B. Kapilevich and B. Litvak, "Optimized microwave sensor for online concentration measurements of binary liquid mixtures," *IEEE Sensors J.*, vol. 11, no. 10, pp. 2611–2616, Oct. 2011.

[31] N. Chudpooti, V. Doychinov, P. Akkaraekthalin, I. D. Robertson, and N. Somjit, "Non-invasive millimeter-wave profiler for surface height measurement of photoresist films," *IEEE Sensors J.*, vol. 18, no. 8, pp. 3174–3182, Apr. 2018.

[32] N. Chudpooti, V. Doychinov, B. Hong, P. Akkaraekthalin, I. Robertson, and N. Somjit, "Multi-modal millimeter-wave sensors for plastic polymer material characterization," *J. Phys. D, Appl. Phys.*, vol. 51, no. 27, Jun. 2018, Art. no. 275103.

[33] K. Grenier, D. Dubuc, P.-E. Poleni, M. Kumemura, H. Toshiyoshi, T. Fujii, and H. Fujita, "Integrated broadband microwave and microfluidic sensor dedicated to bioengineering," *IEEE Trans. Microw. Theory Techn.*, vol. 57, no. 12, pp. 3246–3253, Dec. 2009.

[34] P. Velez, J. Munoz-Enano, K. Grenier, J. Mata-Contreras, D. Dubuc, and F. Martin, "Split ring resonator-based microwave fluidic sensors for electrolyte concentration measurements," *IEEE Sensors J.*, vol. 19, no. 7, pp. 2562–2569, Apr. 2019.

[35] D. J. Rowe, S. al-Malki, A. A. Abduljabar, A. Porch, D. A. Barrow, and C. J. Allender, "Improved split-ring resonator for microfluidic sensing," *IEEE Trans. Microw. Theory Techn.*, vol. 62, no. 3, pp. 689–699, Mar. 2014.

[36] P. Velez, L. Su, K. Grenier, J. Mata-Contreras, D. Dubuc, and F. Martin, "Microwave microfluidic sensor based on a microstrip Splitter/Combiner configuration and split ring resonators (SRRs) for dielectric characterization of liquids," *IEEE Sensors J.*, vol. 17, no. 20, pp. 6589–6598, Oct. 2017.

[37] A. Ebrahimi, W. Withayachumnankul, S. Al-Sarawi, and D. Abbott, "High-sensitivity metamaterial-inspired sensor for microfluidic dielectric characterization," *IEEE Sensors J.*, vol. 14, no. 5, pp. 1345–1351, May 2014.

[38] P. Velez, K. Grenier, J. Mata-Contreras, D. Dubuc, and F. Martin, "Highly-sensitive microwave sensors based on open complementary split ring resonators (OCSRRs) for dielectric characterization and solute concentration measurement in liquids," *IEEE Access*, vol. 6, pp. 48324–48338, 2018.

[39] *CST-MW Studio*, Comput. Simul. Technol., Framingham, MA, USA, 2017.

[40] I. Robertson, N. Somjit, and M. Chongcheawchamnan, *Microwave and Millimeter-Wave Design for Wireless Communications*. Hoboken, NJ, USA: Wiley, 2016.

[41] G. L. Matthael, L. Yong, and E. M. T. Lones, *Miceowave Filters, Impedance-Matching Networks and Coupling Structures*. North Bergen, NJ, USA: Artech House, Nov. 1985.

[42] Pasternack Enterprises. *PE4128 CAD Drawing, SMA Female Connector Solder Attachments 2 Hole Flange Mount Stub. Terminal,.481 inch Hole Spacing,.050 inch Diameter, Gold Plated*. Accessed: Feb. 27, 2020. [Online]. Available: https://www.pasternack.com/images/ProductPDF/PE4128.pdf

[43] A. Ebrahimi, J. Scott, and K. Ghorbani, "Differential sensors using microstrip lines loaded with two split-ring resonators," *IEEE Sensors J.*, vol. 18, no. 14, pp. 5786–5793, Jul. 2018.

[44] A. Ebrahimi, J. Scott, and K. Ghorbani, "Highly sensitive microwave-based biosensor for electrolytic level measurement in water," in *Proc. IEEE Asia–Pacific Microw. Conf. (APMC)*, Singapore, Dec. 2019, pp. 759–761.

NONCHANUTT CHUDPOOTI (Member, IEEE) received the B.Sc. degree (Hons.) in industrial physics and medical instrumentation and the Ph.D. degree in electrical engineering from the King Mongkut's University of Technology North Bangkok, in 2012 and 2018, respectively. He was appointed as a Lecturer at the Department of Industrial Physics and Medical Instrumentation, Faculty of Applied Science, King Mongkut's University of Technology North Bangkok, in 2018. His main research interests include the application of microwave microfluidic sensors, millimeter-wave substrate integrated circuit applications, and substrate integrated waveguide applications. He was a recipient of the Best Presentation Award from the Thailand-Japan Microwave, in 2015 and 2018, and the Young Researcher Encouragement Award, in 2016.

NATTAPONG DUANGRIT (Member, IEEE) was born in Chiang Mai, Thailand, in 1991. He received the B.Eng. degree in electronics and telecommunications engineering from the Rajamangala University of Technology Thanyaburi, in 2015, and the Ph.D. degree from the King Mongkut's University of Technology North Bangkok, in 2019. He is currently working as a Lecturer with the Faculty of Engineering, Rajamangala University of Technology Lanna. His main research interests include application of 3D printing technology for millimeter-wave and THz devices and substrate integrated waveguide applications.

PATCHADAPORN SANGPET was born in Chiang Rai, Thailand, in 1992. She received the bachelor's degree in industrial physics and medical equipment and the master's degree in electrical and computer engineering from the King Mongkut's University of Technology North Bangkok, in 2013 and 2016, respectively, where she is currently pursuing the Ph.D. degree with the Department of Electrical and Computer Engineering. Her research interests include microwave sensor, 5G technology, and the antenna used active feedback devices.

PRAYOOT AKKARAEKTHALIN (Member, IEEE) received the B.Eng. and M.Eng. degrees in electrical engineering from the King Mongkut's University of Technology North Bangkok (KMUTNB), Bangkok, Thailand, in 1986 and 1990, respectively, and the Ph.D. degree from the University of Delaware, Newark, DE, USA, in 1998. From 1986 to 1988, he was a Research and Development Engineer with Microtek Products Company Ltd., Thailand. In 1988, he joined the Department of Electrical Engineering, KMUTNB. He was the Head of the Senior Research Scholar Project which is supported by the Thailand Research Fund, from 2015 to 2017. He has authored or coauthored more than 40 international journals, more than 200 conference papers, and four books/book chapters. His current research interests include RF/microwave circuits, wideband and multiband antennas, telecommunication, and sensor systems. He is a member of IEICE, Japan, ECTI, and the EEAAT Association, Thailand. He was the Chairman of the IEEE MTT/AP/ED Thailand Joint Chapter, from 2007 to 2010, and the Vice President and the President of the ECTI Association, Thailand, from 2012 to 2013 and 2014 to 2015, respectively. He was the Editor-in-Chief of the *ECTI Transactions*, from 2011 to 2013.

B. ULRIK IMBERG received the M.Sc. degree in applied physics and electrical engineering from The Institute of Technology, Linköping University, in 1997. He is currently leading the Huawei Technologies Sweden AB Wireless Technology Planning Team. His research interests include 5G and 6G telecommunication systems and technologies, especially active antennas, antenna-near electronics, and photonics.

IAN D. ROBERTSON (Fellow, IEEE) received the B.Sc. (Eng.) and Ph.D. degrees from the King's College London, London, U.K., in 1984 and 1990, respectively. From 1984 to 1986, he was with the GaAs MMIC Research Group, Plessey Research, Caswell, U.K. Then, he returned to the King's College, initially as a Research Assistant working on the T-SAT project and, then, as a Lecturer leading the MMIC Research Team, where he became a Reader, in 1994. In 1998, he became a Professor of microwave subsystems engineering with the University of Surrey, where he established the Microwave Systems Research Group and was a Founding Member of the Advanced Technology Institute. In 2004, he was appointed as the Centenary Chair of microwave and millimetre-wave circuits with the University of Leeds. He was the Director of learning and teaching, from 2006 to 2011, and the Head of the School, from 2011 to 2016. He was the General Technical Programme Committee Chair of the European Microwave Week, in 2011 and 2016.

NUTAPONG SOMJIT (Senior Member, IEEE) received the Dipl.Ing. (M.Sc.) degree from the Dresden University of Technology, in 2005, and the Ph.D. degree from the KTH Royal Institute of Technology, in 2012.

Then, he returned to Dresden to lead a Research Team in micro-sensors and MEMS ICs for the Chair for Circuit Design and Network Theory. In 2013, he was appointed as a Lecturer (an Assistant Professor) with the School of Electronic and Electrical Engineering, University of Leeds, where he is currently an Associate Professor/Reader. His main research interests include integrated smart high-frequency components, heterogeneous integration, and low-cost micro-fabrication processes. He was appointed as a member of the Engineering, Physical and Space Science Research Panel of the British Council in 2014. He was a recipient of the Best Paper Award (EuMIC prize) at the European MicrowaveWeek in 2009. He was awarded a Graduate Fellowship from the IEEE Microwave Theory and Techniques Society (MTT-S) in 2010 and 2011, and the IEEE Doctoral Research Award from the IEEE Antennas and Propagation Society in 2012. In 2016, he was the Chair of the Student Design Competition for the European Microwave Week. Since 2013, he has been a member of the International Editorial Board of the *International Journal of Applied Science and Technology*. In 2018, he was appointed as an Associate Editor of *IET Electronics Letters*.